Pergamon

Computers & Structures Vol. 50, No. 5, pp. 603–613, 1994

0045-7949/94 $6.00 + 0.00

A STRESS CORRECTION PROCEDURE FOR THE ANALYSIS OF INELASTIC FRAMES UNDER TRANSIENT DYNAMIC LOADS

S. R. MARUR† and T. KANT‡

†CSS Foundation for Research in Finite Elements, B4/4, Vaigai Nagar, Madurai-625 010, India
‡Department of Civil Engineering, Indian Institute of Technology, Powai, Bombay-400 076, India

(*Received* 14 *December* 1992)

Abstract—This paper attempts to present an algorithm (as a set of conditions and equations) for the correction of stresses of both strain-hardening and perfectly-plastic materials, for the analysis of frames under transient dynamic loadings. The validity of the proposed conditions and equations is verified through numerical experiments.

1. INTRODUCTION

Frames subjected to dynamic loads, such as earthquake, blast, etc., undergo inelastic deformations well into the plastic range. The study of the response of frames, in such conditions, would be more realistic, only if the nonlinearities due to material behaviour are taken into account. As these loads are likely to act once or twice on a structure during its life span, design of structures based on elasto-plastic behaviour would be more economical. Thus, nonlinear dynamic analysis is a prelude to achieving both accuracy and economy in the structural design.

In any elasto-plastic analysis, the initiation of yielding in a cross-section can be governed by a yield criterion, formulated either in terms of cross-section stress resultants or Gauss point stresses.

The yield criteria, expressed in terms of axial force and bending moment, generally require an algorithm to bring the drifting force point back to the closed convex yield surface. Toridis and Khozeimeh [1] used von Mises yield criterion based on stress resultants to study the plastic behaviour of each end cross-section of elements of frames subjected to transient loads. And they had to resort to an alogrithm to correct the values of the stress resultants (evaluated based on elastic increments) of elements, deforming plastically. Similarly, Hilmy and Abel [2] made use of a yield criterion, in terms of member end axial force and bending moment, to analyse the nonlinear dynamic behaviour of frames which also required an iterative procedure to control the force point drift from the loading surface. Similarly many algorithms have been reported in the past [3–5] to force the stress point back to the yield surface.

The yield criterion for a plane frame element can also be expressed in terms of its axial and bending stresses (as they are uniaxial in nature) and the yield stress of the material. The shear stress–strain relation, if transverse shear deformation is taken into account, is considered to be elastic [6]. In such a case, the stress point drift will have to be brought back to the stress–strain curve of the material rather than to the yield surface, as in the previous case.

The well-known mechanical sublayer model by White [7] and Besseling [8], models strain-hardening behaviour by assuming each Gauss point to consist of a specified number of sublayers of perfectly-plastic material, which are equally strained, with same elastic modulus but each with a different yield stress. Morris and Fenves [9] used the von Mises yield criterion, in terms of stresses, to determine the initiation of plastic yielding at any point of an element.

Likewise, Nigam [10] applied the same criterion to monitor the starting of plastic flow, within an element of a frame under dynamic loadings. Later on the mechanical sublayer model was adopted by Wu and Witmer [11] for the nonlinear dynamic analysis of structures. Kam and Lin [12] modelled the perfectly-plastic behaviour, in terms of Gauss point stresses, for frames subjected to transient loadings.

When the material is assumed to be perfectly-plastic bringing the stress point back to the stress–strain curve, becomes much simpler, with the conditions used in [11] (Fig. 1). But modelling strain-hardening behaviour is hardly that explicit (Fig. 2).

The sublayer model adopts different yield stresses and a constant known as the 'mechanical sublayer weighing factor' for each perfectly-plastic sublayer in order to model strain-hardening. The concept of a universal stress–strain curve was used in [1] to model the strain-hardening behaviour, wherein the stress is plotted against the plastic component of the strain, evaluated from the actual stress–strain curve of the material.

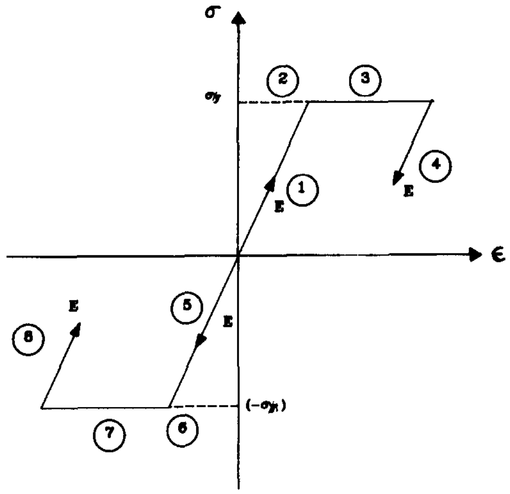

Fig. 1. Stress–strain diagram of a perfectly-plastic material.

If the sublayer model is to be used, then the yield stress and the 'mechanical sublayer weighing factor' for each sublayer of all Gauss points are required at every time-step to calculate the actual member end stress resultants. Again, if the universal stress–strain diagram is to be used, for modelling the strain-hardening effects, it has to be prepared for different kinds of material, from their actual stress–strain diagrams.

Thus, if the formulation of a yield criterion in terms of stress resultants, requires an iterative stress correction algorithm, expressing the same, in terms of Gauss point stresses, on the other hand, involves additional modelling work, as discussed above.

While the interative schemes increase the overall computational effort manyfold, particularly for non-linear transient dynamic analysis using the direct integration schemes, the available methods in terms of stresses, require extra effort for each new type of material likely to be modelled.

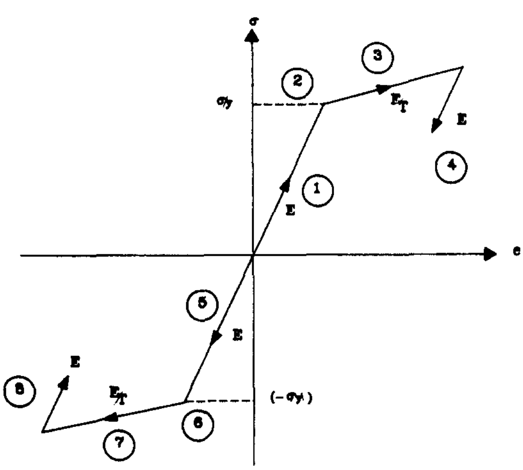

Fig. 2. Stress–strain diagram of a linear strain-hardening material.

Hence, an attempt is made in this study towards a stress correction algorithm in terms of Gauss point stresses (as a set of conditions and correcting equations), which would require neither an iterative stress correction algorithm nor any additional computation, towards evaluating the material dependent parameter(s), would also model both the strain-hardening and perfectly-plastic behaviour and finally, would easily fit into any general purpose finite element code, by incorporating the following features:

(a) the plastic deformations will be measured using only the yield stress (σ_y), Young's modulus (E) and the tangential modulus (E_T) of the material;

(b) the state of stress at any Gauss point will be evaluated by direct comparison with the yield stress of the material; and

(c) a direct and simple procedure will be adopted, to bring the drifting stress point back to the stress–strain curve.

2. THE NEED FOR STRESS CORRECTION

The discrete (with finite elements for spatial discretization) governing equation of dynamic equilibrium

$$[M]\{\ddot{d}\}_{n+1} + [C]\{\dot{d}\}_{n+1} + \{p\}_{n+1} = \{f\}_{n+1}, \quad (1)$$

where $\{p\}_{n+1}$ and $\{f\}_{n+1}$ are the internal and external force vectors, respectively, at time $t = t_{n+1}$, can be expressed in the incremental form as

$$[M]\{\Delta\ddot{d}\}_{n+1} + [C]\{\Delta\dot{d}\}_{n+1} + \{\Delta p\}_{n+1} = \{\Delta f\}_{n+1}, \quad (2)$$

where the incremental acceleration is

$$\{\Delta\ddot{d}\}_{n+1} = \{\ddot{d}\}_{n+1} - \{\ddot{d}\}_n \quad (2a)$$

the incremental velocity is

$$\{\Delta\dot{d}\}_{n+1} = \{\dot{d}\}_{n+1} - \{\dot{d}\}_n, \quad (2b)$$

and the incremental internal and external forces are

$$\{\Delta p\}_{n+1} = \{p\}_{n+1} - \{p\}_n \quad (2c)$$

and

$$\{\Delta f\}_{n+1} = \{f\}_{n+1} - \{f\}_n. \quad (2d)$$

Using the direct integration schemes for the solution of eqn (2), the displacements at any required time-step can be obtained and the incremental local displacement vector of an element at $t = t_{n+1}$ can be given as

$$\{\Delta d_e\}_{n+1} = \{d_e\}_{n+1} - \{d_e\}_n. \quad (3)$$

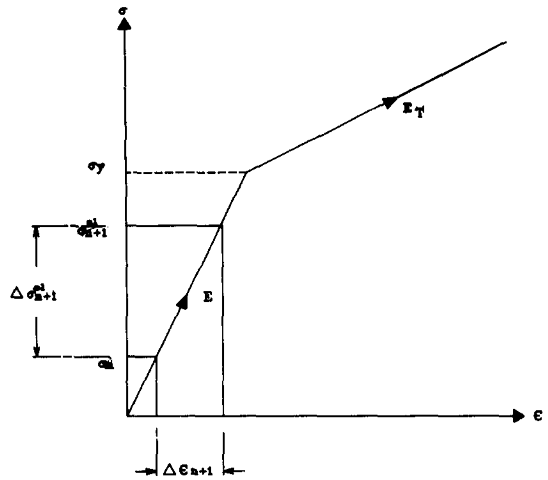

Fig. 3. Elastic loading phase in tension (Case 1).

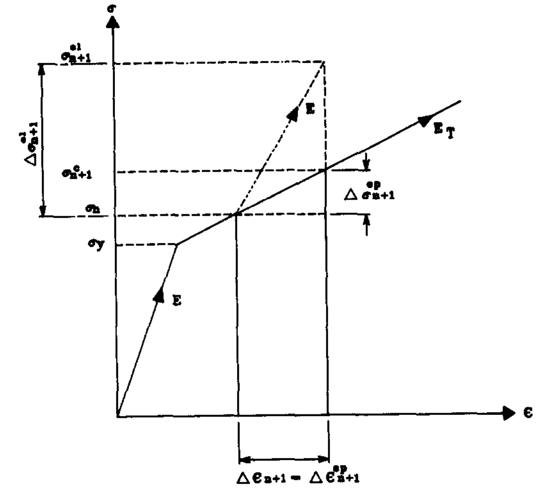

Fig. 5. Yielding in a yielded material in tension (Case 3).

The strain at any Gauss point (ξ, η) in a natural coordinate system can be expressed as

$$\Delta\epsilon(\xi, \eta)_{n+1} = \{B(\xi, \eta)_e\}^T\{\Delta d_e\}_{n+1} \quad (4)$$

where $\{B(\xi, \eta)_e\}$ is the strain–displacement matrix.

The elastic incremental stress at $t = t_{n+1}$ can be calculated as

$$\Delta\sigma(\xi, \eta)^{el}_{n+1} = E\Delta\epsilon(\xi, \eta)_{n+1}, \quad (5)$$

where the superscript *el* denotes that the incremental stress has been calculated based on elastic considerations.

The total stress at $t = t_{n+1}$ is initially given as

$$\sigma(\xi, \eta)^{el}_{n+1} = \Delta\sigma(\xi, \eta)^{el}_{n+1} + \sigma(\xi, \eta)_n, \quad (6)$$

where $\sigma(\xi, \eta)_n$ is the corrected stress at $t = t_n$ and $\sigma(\xi, \eta)^{el}_{n+1}$ is the total stress at the same point at the next time step, evaluated based on an assumed elastic behaviour of the material between $t = t_n$ and t_{n+1}.

During this time interval, however, the material actually could either have remained elastic or gone plastic or become elastic during unloading. So, $\sigma(\xi, \eta)^{el}_{n+1}$ is to be corrected, so as to make it represent the actual state of the material, during that time interval. In other words, the drifting stress point is to be brought back to the stress–strain curve of the material.

If the corrected stress at $t = t_{n+1}$ can be represented as $\sigma(\xi, \eta)^c_{n+1}$ where the superscript c stands for the corrected quantity (the correction procedure is presented later on), then the corrected incremental stress at $t = t_{n+1}$ can be evaluated as

$$\Delta\sigma(\xi, \eta)^c_{n+1} = \sigma(\xi, \eta)^c_{n+1} - \sigma(\xi, \eta)_n \quad (7)$$

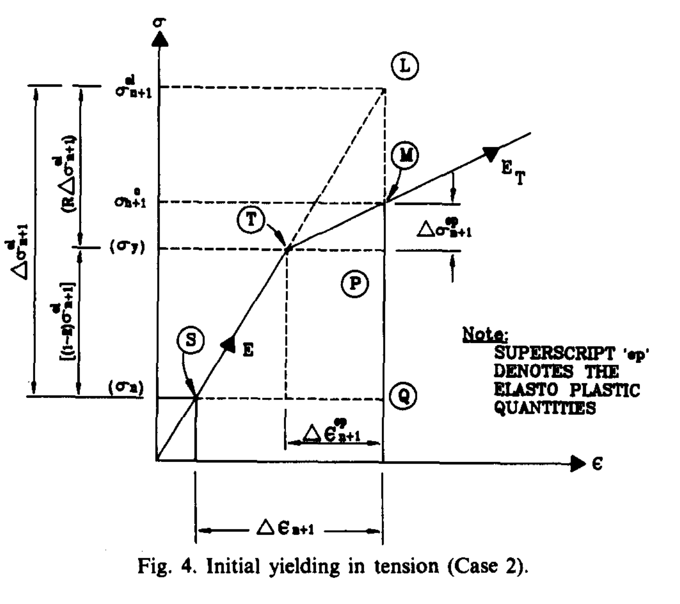

Fig. 4. Initial yielding in tension (Case 2).

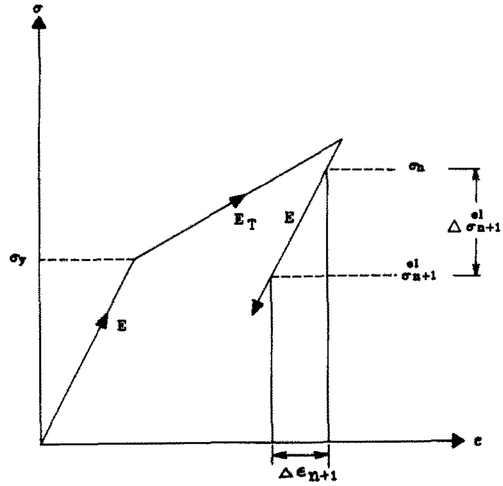

Fig. 6. Elastic unloading in tension (Case 4).

which might be used for evaluating the internal resisting force vector as

$$\{\Delta p_e\}_{n+1} = \int_{V_e} \{B(\xi,\eta)_e\}^T \Delta\sigma(\xi,\eta)^c_{n+1}\,\mathrm{d}v \qquad (8)$$

which in turn can be used to evaluate vector of displacements at the next time step.

3. PROPOSED STRESS CORRECTION CONDITIONS AND EQUATIONS FOR BOTH THE STRAIN-HARDENING AND PERFECTLY-PLASTIC MATERIAL MODELS

Along the lines of the concepts, available in [11] for a perfectly-plastic material, at any Gauss point sublayer under dynamic loadings and in [6], for strain-hardening materials under static loadings only, a set of conditions and equations for both types of material models under dynamic loadings are proposed.

For the sake of simplicity, the stress at a point may be denoted as σ^{el}_{n+1} and σ_n, the strain as ϵ_{n+1} and

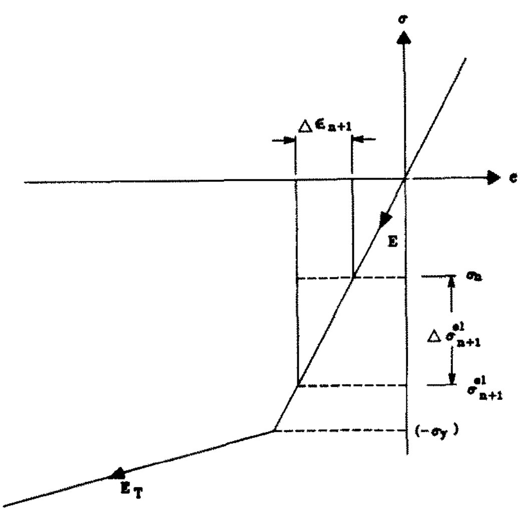

Fig. 7. Elastic loading in compression (Case 5).

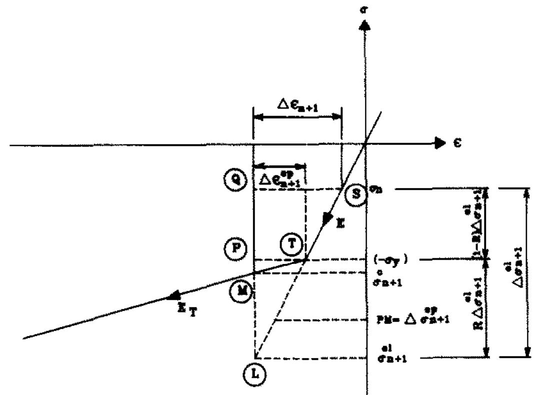

Fig. 8. Initial yielding in compression (Case 6).

the incremental stress as $\Delta\sigma^{el}_{n+1}$, dropping (ξ,η) in the following discussion.

The complete cycle of loading, strain-hardening and unloading in both tension and compression due to bending, is taken in to account while deriving the conditions.

Case 1: *elastic loading in tension*

The elastic loading conditions as shown in Fig. 3 can be said to exist during a particular time interval, if

$$\sigma_n > 0, \quad \sigma_n < \sigma_y, \quad \sigma^{el}_{n+1} \leqslant \sigma_y, \text{ and } \sigma^{el}_{n+1} > \sigma_n \qquad (9)$$

and the corrected stress can be expressed as

$$\sigma^c_{n+1} = \sigma^{el}_{n+1}. \qquad (10)$$

Case 2: *strain hardening in tension—initial yielding.*

If the yielding takes place during the time interval between $t = t_{n+1}$ and $t = t_n$, known as initial yielding, then it can be expressed by the condition

$$\sigma_n > 0, \quad \sigma_n < \sigma_y, \quad \sigma^{el}_{n+1} > \sigma_y, \text{ and } \sigma^{el}_{n+1} > \sigma_n. \qquad (11)$$

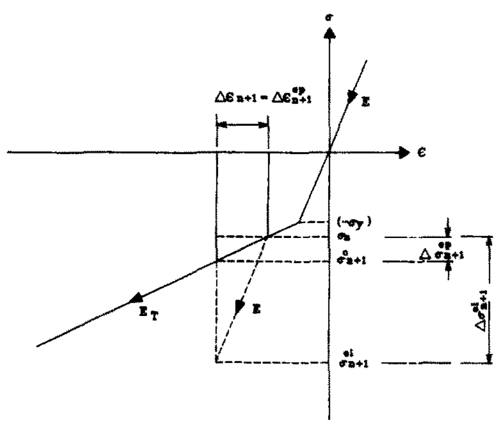

Fig. 9. Yielding in a yielded material in compression (Case 7).

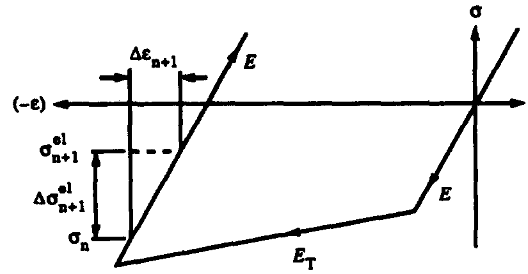

Fig. 10. Elastic unloading in compression (Case 8).

The stress σ^{el}_{n+1}, denoted in Fig. 4 by the point L is to be brought back to the point M on the stress–strain curve, in order to make it represent the true state of the material stress. A constant R can be defined with respect to the above figure as

$$R = LP/LQ = (\sigma^{el}_{n+1} - \sigma_y)/(\sigma^{el}_{n+1} - \sigma_n). \quad (12)$$

The plastic component of incremental strain at $t = t_{n+1}$ is given as

$$\Delta\epsilon^{ep}_{n+1} = TP = R\Delta\epsilon_{n+1} \quad (13)$$

and the corresponding incremental plastic stress component is evaluated as

$$\Delta\sigma^{ep}_{n+1} = PM = E_T R \Delta\epsilon_{n+1}. \quad (14)$$

The difference between σ_y and σ_n, denoted by PQ can be given as

$$PQ = (1 - R)\Delta\sigma^{el}_{n+1}. \quad (15)$$

Using eqns (14) and (15), the corrected stress at $t = t_{n+1}$ can be expressed as

$$\sigma^{c}_{n+1} = \sigma_n + (1 - R)\Delta\sigma^{el}_{n+1} + RE_T\Delta\epsilon_{n+1}. \quad (16)$$

Case 3: strain hardening in tension—previously yielded.

When the material yields before the time step $t = t_n$ as shown in Fig. 5, the state of stress can be expressed by the condition

$$\sigma_n \geq \sigma_y, \quad \sigma^{el}_{n+1} > \sigma_y, \text{ and } \sigma^{el}_{n+1} > \sigma_n. \quad (17)$$

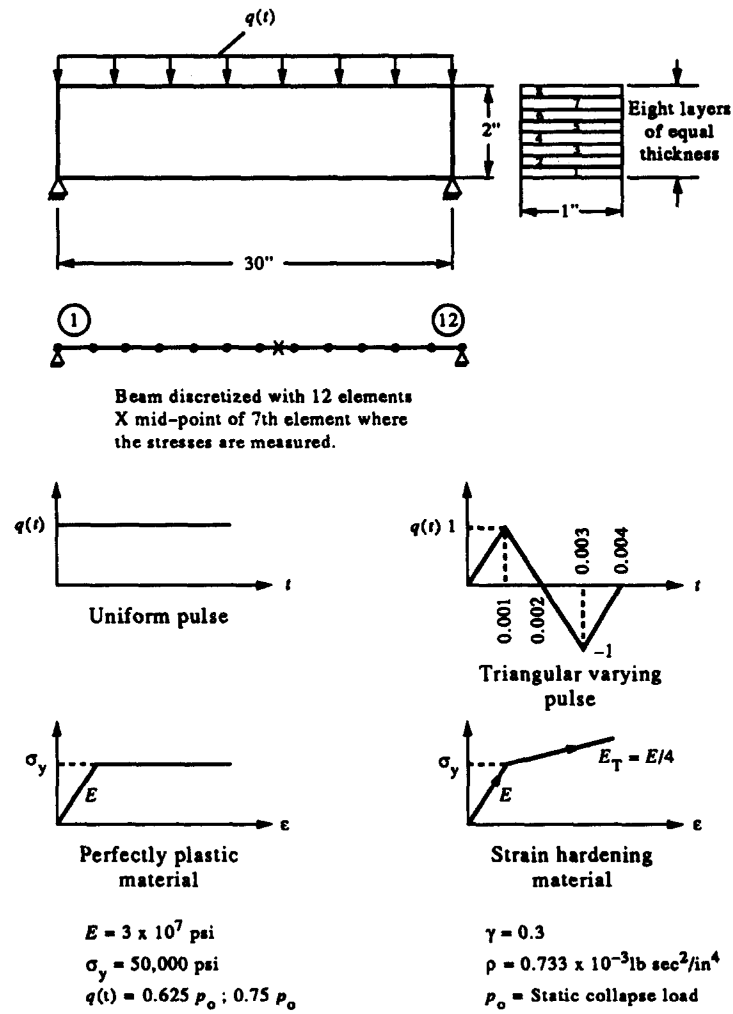

Fig. 11. A simply supported beam with loading functions and material models.

It can be seen from Fig. 5 that for a yielded material, the constant R becomes unity and the corrected stress can be expressed as

$$\sigma^c_{n+1} = \sigma_n + E_T \Delta\epsilon_{n+1}. \quad (18)$$

Case 4: elastic unloading in tension

The unloading takes place elastically as shown in Fig. 6 and can be expressed mathematically as

$$\sigma_n > 0, \quad \sigma_n > (-\sigma_y), \quad \sigma^{el}_{n+1} \geqslant (-\sigma_y), \text{ and } \sigma^{el}_{n+1} < \sigma_n \quad (19)$$

and the corrected stress can be given by eqn (10).

Case 5: elastic loading in compression

The elastic loading in compression as shown in Fig. 7 can be expressed as

$$\sigma_n < 0, \quad \sigma_n > (-\sigma_y), \quad \sigma^{el}_{n+1} \geqslant (-\sigma_y), \quad \text{and } \sigma^{el}_{n+1} < \sigma_n \quad (20)$$

and the corrected stress can be given by eqn (10).

Case 6: strain hardening in compression—initial yielding

When the yielding in compression takes place as shown in Fig. 8, during the particular time interval, between t_n and t_{n+1}, the state of stress can be given as

$$\sigma_n < 0, \quad \sigma_n > (-\sigma_y), \quad \sigma^{el}_{n+1} < (-\sigma_y), \quad \text{and } \sigma^{el}_{n+1} < \sigma_n \quad (21)$$

and the corrected stress is given by eqn (16).

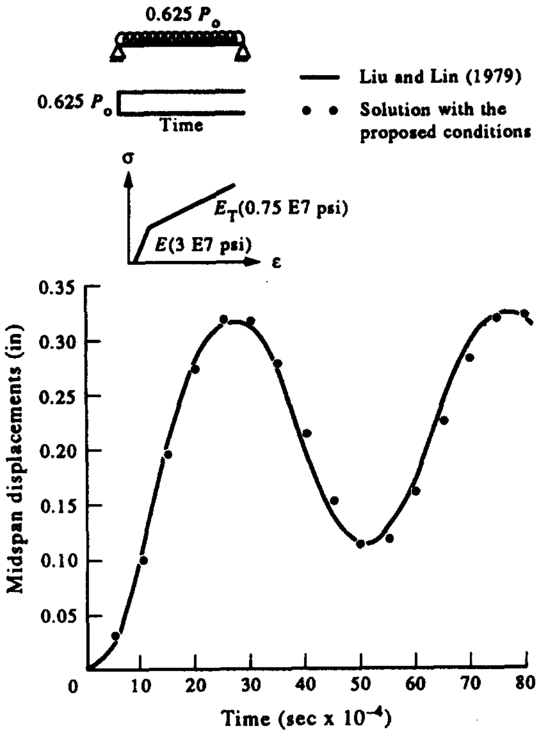

Fig. 12. Elasto-plastic midspan displacements of a simply supported beam with strain-hardening effect.

Case 7: strain hardening in compression—previously yielded

When the material has yielded before $t = t_n$ as in Fig. 9, the state of stress can be expressed as

$$\sigma_n \leqslant (-\sigma_y), \quad \sigma^{el}_{n+1} < (-\sigma_y) \text{ and } \sigma^{el}_{n+1} < \sigma_n \quad (22)$$

and the corrected stress is given by eqn (18).

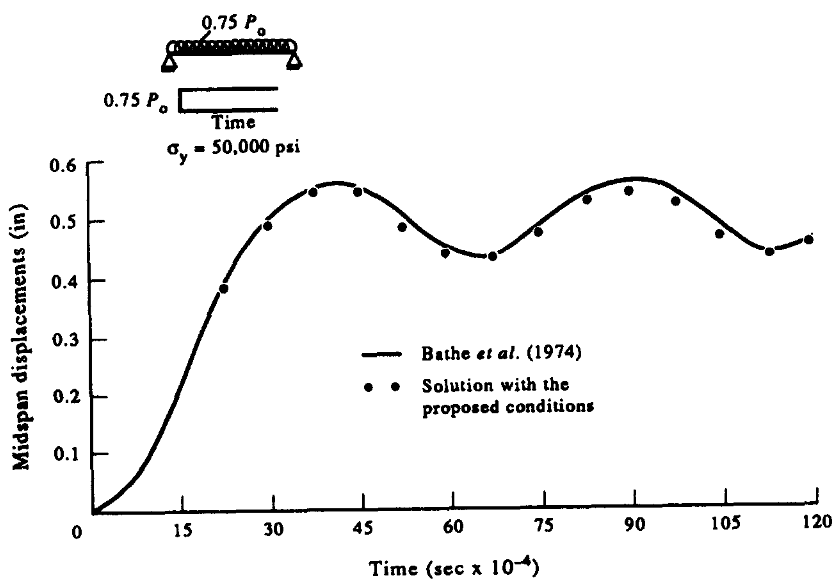

Fig. 13. Elasto-plastic midpsan deflections of a simply supported beam.

Case 8: *elastic unloading in compression*

The unloading which takes place elastically, after yielding in compression as shown in Fig. 10 can be expressed as

$$\sigma_n < 0, \quad \sigma_n < \sigma_y, \quad \sigma_{n+1}^{el} \leqslant \sigma_y, \text{ and } \sigma_{n+1}^{el} > \sigma_n \quad (23)$$

and the corresponding corrected stress by eqn (10).

The stress at any point representing the actual state of the material at $t = t_{n+1}$ could be obtained from eqns (9)–(23), which cover all the possible phases of the stress–strain curve.

Moreover, it can be seen that, by making the value of E_T equal to zero in the eqns (16) and (18), the corrected stresses for the perfectly plastic material can directly be obtained. Thus, the proposed conditions and equations can effectively be used for both strain-hardening and perfectly-plastic material models.

4. NUMERICAL EXPERIMENTS

In order to validate, the proposed conditions and equations through numerical experiments, some examples of beams and frames with different material models and loadings are analysed, on an IBM-compatible 386 graphic work-station, on a DOS platform using double precision.

Example 1

A simply supported beam analysed by Bathe *et al.* [13] using von Mises yield criterion and later on by Liu and Lin [14] is considered here to verify the proposed conditions and equations for different types of material models.

The beam is subjected to a uniformly distributed dynamic step pressure of $0.625p_0$, where p_0 is the static collapse load. The mass of the beam is taken to be 0.733×10^{-3} lb sec^2/in^4, while Poisson's ratio γ is 0.3 and the depth and breadth of a 30 in long beam are 2 in and 1 in respectively. The beam has been discretized by 12, two-noded linear elements of Hughes *et al.* [15].

The cross-section of the beam is split into eight layers of equal thickness for evaluating the stesses. The explicit central difference technique is used for the time history analysis. The yield stress of the material is taken to be 50,000 psi and the tangential modulus is set equal to one fourth of the value of Young's modulus of 3×10^7 psi.

The solution using the proposed conditions along with that of [14] is plotted in Fig. 12 and the close agreement between the two can be observed. This beam for another load of $0.75p_0$, with the perfectly-plastic material and von Mises criterion has been analysed earlier [13]. That result is plotted with that obtained from the proposed conditions, in Fig. 13. The agreement between the two results validates the applicability of the proposed conditions for both types of materials.

The same beam, with perfectly-plastic and strain-hardening material models, is again subjected to $0.75p_0$ load varying as an uniform pulse as well as a triangularly varying pulse as shown in Fig. 11. The distribution of stresses across the depth at different time-steps are shown in Tables 1–4. The numbers given in parentheses, referred to as the index values in the following discussion, correspond to different cases of material states as discussed in the previous section.

From Table 1, let us consider a layer, say 4. It remains elastic until 0.0035 sec, then becomes plastic and then unloading sets in at 0.00475 sec. The stress increases again elastically at 0.00575 sec, followed by unloading and again an increase at 0.0075 sec. Similarly the chronological change in the material state of different layers can be observed, using the indices of this table.

Table 1. Cross-sectional stress distribution of a beam with perfectly-plastic material, subjected to uniform pulse

Layer No.	Stress in psi at time (in sec)							
	0.500E − 3	0.150E − 2	0.350E − 2	0.475E − 2	0.575E − 2	0.675E − 2	0.750E − 2	0.800E − 2
8	−0.9391E4 (5)	−0.5000E5 (7)	−0.5000E5 (7)	−0.4415E5 (8)	−0.2473E5 (5)	−0.1766E5 (8)	−0.2787E5 (5)	−0.3702E5 (5)
7	−0.6708E4 (5)	−0.4860E5 (5)	−0.5000E5 (7)	−0.4582E5 (8)	−0.3195E5 (5)	−0.2690E5 (8)	−0.3419E5 (5)	−0.4073E5 (5)
6	−0.4025E4 (5)	−0.2916E5 (5)	−0.5000E5 (7)	−0.4749E5 (8)	−0.3917E5 (5)	−0.3614E5 (8)	−0.4052E5 (5)	−0.4444E5 (5)
5	−0.1342E4 (5)	−0.9721E4 (5)	−0.3789E5 (5)	−0.3872E5 (8)	−0.3594E5 (5)	−0.3493E5 (8)	−0.3639E5 (5)	−0.3770E5 (5)
4	0.1342E4 (1)	0.9721E4 (1)	0.3789E5 (1)	0.3872E5 (4)	0.3594E5 (1)	0.3493E5 (4)	0.3639E5 (1)	0.3770E5 (1)
3	0.4025E4 (1)	0.2916E5 (1)	0.5000E5 (3)	0.4749E5 (4)	0.3917E5 (1)	0.3614E5 (4)	0.4052E5 (1)	0.4444E5 (1)
2	0.6708E4 (1)	0.4860E5 (1)	0.5000E5 (3)	0.4582E5 (4)	0.3195E5 (1)	0.2690E5 (4)	0.3419E5 (1)	0.4073E5 (1)
1	0.9391E4 (1)	0.5000E5 (3)	0.5000E5 (3)	0.4415E5 (4)	0.2473E5 (1)	0.1766E5 (4)	0.2787E5 (1)	0.3702E5 (1)

Table 2. Cross-sectional stress distribution of a beam with perfectly plastic material, subjected to triangular pulse

Layer No.	Stress in psi at time (in sec)												
	0.500E − 3	0.200E − 2	0.275E − 2	0.325E − 2	0.350E − 2	0.425E − 2	0.500E − 2	0.600E − 2	0.650E − 2	0.700E − 2	0.725E − 2	0.750E − 2	0.800E − 2
8	−0.8194E3 (5)	−0.5000E5 (7)	−0.3465E5 (8)	0.1024E5 (1)	0.3864E5 (1)	0.5000E5 (3)	0.4817E5 (4)	−0.1047E5 (5)	−0.4994E5 (5)	−0.5000E5 (7)	−0.4909E5 (8)	−0.500E5 (7)	−0.3366E5 (8)
7	−0.5853E3 (5)	−0.3951E5 (5)	−0.3252E5 (8)	−0.4575E3 (8)	0.1983E5 (1)	0.5000E5 (3)	0.4869E5 (4)	0.6807E4 (4)	−0.2139E5 (5)	−0.5000E5 (7)	−0.4935E5 (8)	−0.5000E5 (7)	−0.3833E5 (8)
6	−0.3512E3 (5)	−0.2371E5 (5)	−0.1951E5 (8)	−0.2745E3 (8)	0.1190E5 (1)	0.5000E5 (3)	0.4921E5 (4)	0.2408E5 (4)	0.7167E4 (4)	−0.1044E5 (5)	−0.1172E5 (8)	−0.1362E5 (5)	−0.7172E4 (8)
5	−0.1171E3 (5)	−0.7903E4 (5)	−0.6503E4 (8)	−0.9149E2 (8)	0.3966E4 (1)	0.2294E5 (1)	0.2823E5 (4)	0.1985E5 (4)	0.1422E5 (4)	0.8346E4 (4)	0.7919E4 (1)	0.7286E4 (4)	0.9436E4 (1)
4	0.1171E3 (1)	0.7903E4 (1)	0.6503E4 (4)	0.9149E2 (4)	−0.3966E4 (5)	−0.2294E5 (5)	−0.2823E5 (8)	−0.1985E5 (8)	−0.1422E5 (8)	−0.8346E4 (8)	−0.7919E4 (5)	−0.7286E4 (8)	−0.9436E4 (5)
3	0.3512E3 (1)	0.2371E5 (1)	0.1951E5 (4)	0.2745E3 (4)	−0.1190E5 (5)	−0.5000E5 (7)	−0.4921E5 (8)	−0.2408E5 (8)	−0.7167E4 (8)	+0.1044E5 (1)	0.1172E5 (4)	0.1362E5 (1)	0.7172E4 (4)
2	0.5853E3 (1)	0.3951E5 (1)	0.3252E5 (4)	0.4575E3 (4)	−0.1983E5 (5)	−0.5000E5 (7)	−0.4869E5 (8)	−0.6807E4 (8)	0.2139E5 (1)	0.5000E5 (3)	0.4935E5 (4)	0.5000E5 (3)	0.3833E5 (4)
1	0.8194E3 (1)	0.5000E5 (3)	0.3465E5 (4)	−0.1024E5 (5)	−0.3864E5 (5)	−0.5000E5 (7)	−0.4817E5 (8)	0.1047E5 (1)	0.4994E5 (1)	0.5000E5 (3)	0.4909E5 (4)	0.5000E5 (3)	0.3366E5 (4)

Table 3. Cross-sectional stress distribution of a beam with strain-hardening material, subjected to uniform pulse

Layer No.	Stress in psi at time (in sec)									
	0.500E − 3	0.125E − 2	0.175E − 2	0.225E − 2	0.250E − 2	0.300E − 2	0.425E − 2	0.625E − 2	0.725E − 2	0.800E − 2
8	−0.9391E4 (5)	−0.5023E5 (7)	−0.6100E5 (7)	−0.6668E5 (7)	−0.7030E5 (7)	−0.6992E5 (7)	−0.3873E5 (8)	−0.2167E5 (5)	−0.5338E5 (7)	−0.5878E5 (7)
7	−0.6708E4 (5)	−0.3636E5 (5)	−0.5429E5 (7)	−0.5834E5 (7)	−0.6093E5 (7)	−0.6066E5 (7)	−0.3838E5 (8)	−0.2619E5 (5)	−0.5152E5 (7)	−0.5538E5 (7)
6	−0.4025E4 (5)	−0.2181E5 (5)	−0.4029E5 (5)	−0.5001E5 (6)	−0.5156E5 (7)	−0.5139E5 (7)	−0.3803E5 (8)	−0.3071E5 (5)	−0.4866E5 (5)	−0.5198E5 (7)
5	−0.1342E4 (5)	−0.7272E4 (5)	−0.1343E5 (5)	−0.1668E5 (5)	−0.1874E5 (5)	−0.1922E5 (5)	−0.1510E5 (8)	−0.1266E5 (5)	−0.1864E5 (5)	−0.2186E5 (5)
4	0.1342E4 (1)	0.7272E4 (1)	0.1343E5 (1)	0.1668E5 (1)	0.1874E5 (1)	0.1922E5 (1)	0.1510E5 (4)	0.1266E5 (1)	0.1864E5 (1)	0.2186E5 (1)
3	0.4025E4 (1)	0.2181E5 (1)	0.4029E5 (1)	0.5001E5 (2)	0.5156E5 (3)	0.5139E5 (3)	0.3803E5 (4)	0.3071E5 (1)	0.4866E5 (1)	0.5198E5 (3)
2	0.6708E4 (1)	0.3636E5 (1)	0.5429E5 (3)	0.5834E5 (3)	0.6093E5 (3)	0.6066E5 (3)	0.3838E5 (4)	0.2169E5 (1)	0.5152E5 (3)	0.5538E5 (3)
1	0.9391E4 (1)	0.5023E5 (3)	0.6100E5 (3)	0.6668E5 (3)	0.7030E5 (3)	0.6992E5 (3)	0.3873E5 (4)	0.2167E5 (1)	0.5338E5 (3)	0.5878E5 (3)

Table 4. Cross-sectional stress distribution of a beam with strain-hardening material, subjected to triangular pulse

Layer No.	Stress in psi at time (in sec)												
	0.250E − 3	0.100E − 2	0.200E − 2	0.275E − 2	0.325E − 2	0.375E − 2	0.425E − 2	0.500E − 2	0.600E − 2	0.650E − 2	0.700E − 2	0.725E − 2	0.800E − 2
8	0.8887E2	−0.1088E5	−0.5121E5	−0.3693E5	0.8197E4	0.5464E5	0.6869E5	0.6164E5	−0.1881E5	−0.5408E5	−0.6230E5	−0.6235E5	−0.3677E5
	(1)	(5)	(7)	(8)	(1)	(3)	(3)	(4)	(5)	(7)	(8)	(7)	(8)
7	0.6348E2	−0.7771E4	−0.3917E5	−0.3113E5	0.1099E4	0.4420E5	0.5859E5	0.5355E5	−0.3909E4	−0.3785E5	−0.5283E5	−0.5287E5	−0.3460E5
	(1)	(5)	(5)	(8)	(1)	(1)	(3)	(4)	(5)	(5)	(8)	(7)	(8)
6	0.3809E2	−0.4663E4	−0.2350E5	−0.1868E5	0.6597E3	0.2652E5	0.5016E5	0.4713E5	0.1265E5	−0.7710E4	−0.2229E5	−0.2371E5	−0.1357E5
	(1)	(5)	(5)	(8)	(1)	(1)	(3)	(4)	(4)	(5)	(8)	(5)	(8)
5	0.1270E2	−0.1554E4	−0.7833E4	−0.6227E4	0.2199E3	0.8841E4	0.1687E5	0.1718E5	0.5683E4	−0.1105E4	−0.5966E4	−0.6438E4	−0.3059E4
	(1)	(5)	(5)	(8)	(1)	(1)	(1)	(4)	(4)	(5)	(8)	(5)	(8)
4	−0.1270E2	0.1554E4	0.7833E4	0.6227E4	−0.2199E3	−0.8841E4	−0.1687E5	−0.1718E5	−0.5683E4	0.1105E4	0.5966E4	0.6438E4	0.3059E4
	(5)	(1)	(1)	(4)	(5)	(5)	(5)	(8)	(8)	(1)	(4)	(1)	(4)
3	−0.3809E2	0.4663E4	0.2350E5	0.1868E5	−0.6597E3	−0.2652E5	−0.5016E5	−0.4713E5	−0.1265E5	0.7710E4	0.2229E5	0.2371E5	0.1357E5
	(5)	(1)	(1)	(4)	(5)	(5)	(7)	(8)	(8)	(1)	(4)	(1)	(4)
2	−0.6348E2	0.7771E4	0.3917E5	0.3113E5	−0.1099E4	−0.4420E5	−0.5859E5	−0.5355E5	0.3909E4	0.3785E5	0.5283E5	0.5287E5	0.3460E5
	(5)	(1)	(1)	(4)	(5)	(5)	(7)	(8)	(1)	(1)	(4)	(3)	(4)
1	−0.8887E2	0.1088E5	0.5121E5	0.3693E5	−0.8197E4	−0.5464E5	−0.6869E5	−0.6164E5	0.1881E5	0.5408E5	0.6230E5	0.6235E5	0.3677E5
	(5)	(1)	(3)	(4)	(5)	(7)	(7)	(8)	(1)	(3)	(4)	(3)	(4)

The stress distribution for the triangular load is given in Table 2. In layer 1, the material becomes plastic at 0.002 sec followed by unloading. Due to the variation in the direction of the triangular load, the stresses are also bound to reverse from tension to compression and vice cersa. This can be observed from the index value of 5 at 0.00325 sec, and subsequently the material becomes plastic and then the unloading sets in. The stress at 0.006 sec, shows the elastic phase in tension again and goes on to become plastic at 0.007 sec.

From Table 3, if any specific layer, say 3 is considered, it can be seen that the stresses become plastic at 0.00225 sec (as represented by index value of 2), remain plastic until 0.003 sec, followed by unloading and subsequent reloading at 0.00625 sec. A similar pattern can be observed for other layers as well.

For the top layer 8, in Table 4, the material from elastic loading at 0.001 sec in compression, transforms to plastic at 0.002 sec and then the unloading phase follows. The material enters into tensile region at 0.00325 sec, due to the change in the direction of the triangular pulse. After becoming plastic at 0.00425 sec, it unloads and enters the compressive loading at 0.006 sec.

Thus it can be seen that, using the proposed conditions/indices, the different states of material—elastic loading, plastification and unloading in both tension and compression, can clearly be identified and monitored as these conditions correspond to eight distinct material states.

Example 2

Toridis and Khozeimeh [1] had studied a single storeyed frame, with the masses lumped at eight points as shown in Fig. 14, with the actual lumped masses multiplied by a factor of 625, to make the fundamental frequency of the frame very close to that of actual buildings and used von Mises–Hencky yield criterion along with the Reuss–von Mises plastic flow rule. The frame discretized by nine c^1 elements, keeping the position of lumped mass of the reference frame as the nodes, has been analysed here using central difference scheme. The yield stress is taken to be 68,000 psi, Young's modulus as 0.3×10^8 psi and the tangent modulus as 0.3×10^7 psi.

The response history using the proposed conditions along with the output of the reference authors in Fig. 15, shows the close agreement between the two.

5. CONCLUSIONS

A set of conditions and equations are proposed for the stress correction of both the strain-hardening and perfectly-plastic materials, for the analysis of beams and frames. These were found to yield results very

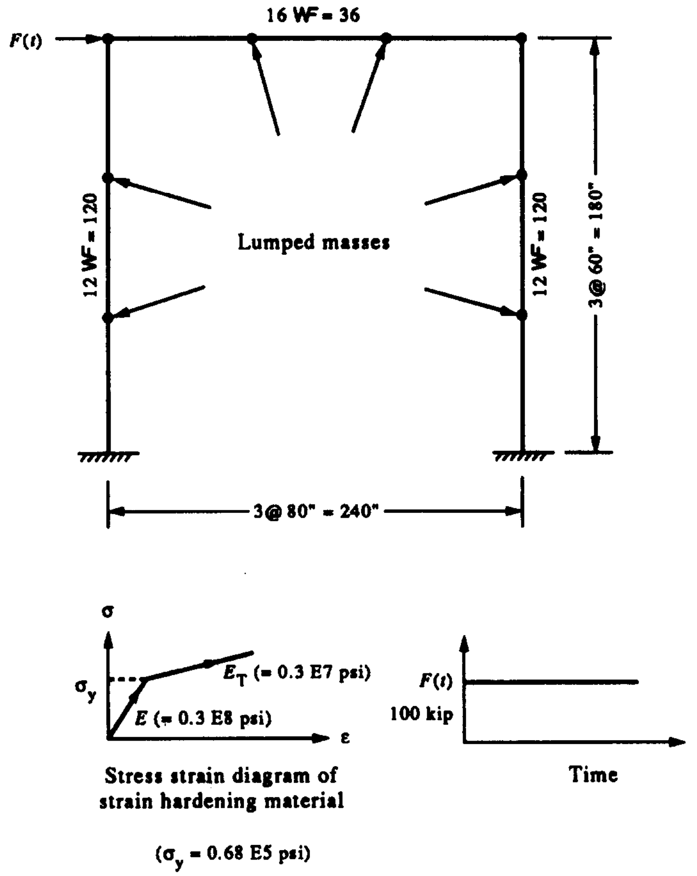

Fig. 14. Rectangular frame with lateral load and strain hardening material model.

much closer to those available in the literature, after the numerical experiments. These conditions and equations can be directly incorporated into an existing computer source code for materially nonlinear transient dynamic analysis of framed structures.

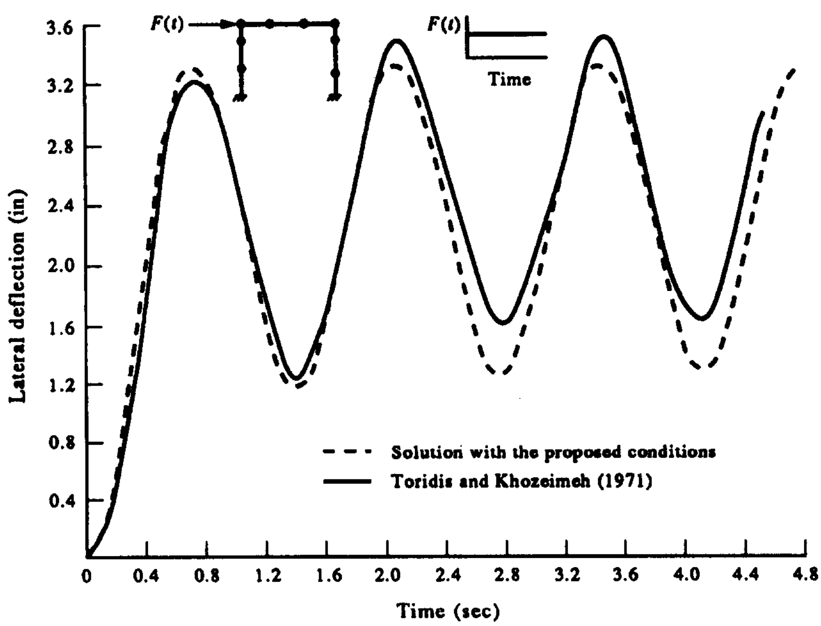

Fig. 15. Time history of elasto-plastic deflection of point of application of load.

REFERENCES

1. T. G. Toridis and K. Khozeimeh, Inelastic response of frames to dynamic loads. *ASCE, J. Struct. Div.* **97**, 847–863 (1971).
2. S. I. Hilmy and J. F. Abel, Material and geometric nonlinear dynamic analysis of steel frames using computer graphics. *Comput. Struct.* **21**, 825–840 (1985).
3. J. G. Orbinson, W. McGuire and J. F. Abel, Yield surface applications in nonlinear steel frame analysis. *Comput. Meth. appl. Mech. Engng* **33**, 557–573 (1982).
4. E. Bozzo and L. Gambarotta, Inelastic analysis of steel frames for multistorey buildings. *Comput. Struct.* **20**, 707–713 (1985).
5. M. B. Wong and T. F. Loi, Yield surface linearization in elasto plastic analysis. *Comput. Struct.* **26**, 951–956 (1987).
6. D. R. J. Owen and E. Hinton, *Finite Elements in Plasticity—Theory and Practice*. Pineridge Press, Swansea (1980).
7. G. N. White, Jr, Application of the theory of perfectly plastic solids to stress analysis of strain hardening solids. Technical Report 51, Brown University, Providence, RI (1950).
8. J. F. Besseling, A theory of plastic flow for anisotropic hardening in plastic deformation of an initially isotropic material. Report S.410, National Aeronautical Research Institute, Amsterdam (1953).
9. G. A. Morris and S. J. Fenves, A general procedure for the analysis of elastic and plastic frame works. Structural Research Series No. 305, Department of Civil Engineering, University of Illinois, IL (1967).
10. N. C. Nigam, Yielding in framed structures under dynamic loads. Ph.D. thesis, California Institute of Technology, Pasadena (1968).
11. R. W. H. Wu and E. A. Witmer, Finite element analysis of large elastic–plastic transient deformations of simple structures. *AIAA Jnl* **9**, 1719–1724 (1971).
12. T. Y. Kam and S. C. Lin, Nonlinear dynamic analysis of inelastic steel plane frames. *Comput. Struct.* **28**, 535–542 (1988).
13. K. J. Bathe, H. Ozdemir and E. L. Wilson, Static and dynamic geometric and material nonlinear analysis. Report No. UCSESM 74-4, University of California, Berkeley (1974).
14. S. C. Liu and T. H. Lin, Elasto-plastic analysis of structures using known elastic solutions. *Earthquake Engng Struct. Dyn.* **7**, 147–160 (1979).
15. T. J. R. Hughes, R. L. Taylor and S. Kanoknukulchai, A simple and efficient finite element for bending. *Int. J. Numer. Meth. Engng* **11**, 1529–1543 (1977).